Intelligence & Robotics

Research Article

Check for updates

Adaptive prescribed performance tracking control for underactuated unmanned surface ships with input quantization

Jiaming Zhang[1], Xiang Liu[1], Xin Wang[1], Yang Wang[2], Yueying Wang[1]

[1]College of Mechatronics Engineering and Automation, Shanghai University, Shanghai 200444, China.
[2]Naval Equipment Department, Marine Equipment Project Management Center, Beijing 1100036, China.

Correspondence to: Prof. Yueying Wang, College of Mechatronics Engineering and Automation, Shanghai University, Shangdalu99, Baoshan District, Shanghai 200444, China. E-mail: wyy676@126.com; Dr. Yang Wang, Naval Equipment Department, Marine Equip-ment Project Management Center, No. 5, East Street, Fengtai District, Beijing 100071, China. E-mail: wallace998@sina.cn

Abstract

This article investigates the preset performance trajectory tracking control problem of underactuated unmanned surface ships with model uncertainty, unknown external environmental disturbances, and input quantization effects. We consider the non-diagonal damping matrix and mass matrix to satisfy the actual dynamics model of underactuated unmanned surface ships. By adding a hysteresis quantizer, the control method proposed in this article effectively reduces the quantization error. Neural networks are employed to approach the unknown environmental disturbance of underactuated unmanned surface ships. Using the error transformation function, the constrained control problem is transformed into an unconstrained one to ensure the preset performance of tracking errors. This paper verifies the superiority and effectiveness of the proposed control method through Lyapunov stability analysis.

Keywords: Underactuated unmanned surface ships, trajectory tracking control, prescribed performance, neural networks

1. INTRODUCTION

Recently, underactuated unmanned surface ships have gained widespread usage across many Marine engineering fields. They hold high application value in Marine tasks such as ocean exploration, water quality moni-

toring, and Marine search and rescue, prompting extensive scholarly research. Trajectory tracking control technology is important for these vessels, enabling them to move along the desired trajectory while ensuring satisfactory performance. However, the dynamics of these ships are time-varying, nonlinear, and often subject to complex ocean disturbances such as currents, waves, and tides. Despite many challenges, some control methods have been proposed to effectively reduce the influence of external unknown interference and model uncertainty, such as sliding mode control[1–3], backstepping adaptive control[4–6], and neural network-based control[7–13].

Due to complex unknown external disturbances and highly coupled nonlinear dynamics in ocean engineering, it is very important to obtain accurate mathematical models of underactuated unmanned surface ships. Only by acquiring accurate model information can some model-related control methods be effective. Several adaptive neural network control design techniques have been proposed in recent years to solve the model uncertainty-related problems of underactuated unmanned surface ships. In ref[13], the high-gain observer was used to estimate the unmeasurable state of ship dynamics. When partial PE conditions are satisfied, the proposed adaptive neural network controller can acquire uncertain ship dynamics knowledge in the stable process and store the learned knowledge in the memory. An adaptive neural network controller was designed in ref[14], which uses the obstacle Lyapunov function (BLF) and combines the backstepping method with adaptive feedback approximation technology to verb the trajectory tracking control problem of fully driven unmanned surface ships with multiple output constraints. In ref[15], by introducing an error transformation function, the constrained tracking control of the original ship is transformed into a stabilizing control of an unconstrained system. Then, a radial basis function neural network (RBFNN) is used to approximate the unknown ship dynamics, and a stable adaptive neural network control is proposed. While ensuring the ultimate boundedness of all signals in the closed-loop system, the improved control performance of fast-tracking convergence speed and low computational complexity is achieved. For a class of multi-input systems with all-state constraints, an adaptive neural network controller is designed in ref[16], which uses the Moor-Penrose generalized inverse matrix to avoid violation of all-state constraints and deal with uncertainty and unknown interference of the system. This paper will use adaptive neural networks to solve problems such as model uncertainty and external interference.

However, in addition to the above model uncertainty and complex external interference, we also need to constrain the tracking error of underactuated unmanned surface ships from the perspective of performance and system safety. In the actual voyage, if these ships exceed the output constraint, they may collide with obstacles such as reefs in the ocean, resulting in reduced control performance and control failure. In addition, if the track tracking error of the surface unmanned ship exceeds the specified boundedness, then the transformed error becomes a meaningless value, which will cause the surface unmanned ship to actively stop working for better self-protection. Therefore, the guaranteed transient performance can improve the security and stability of the system. In ref[17], the tracking control issue of unmanned underwater vehicles (UUV) was studied, and the transient and steady-state characteristics were specified. A new tracking controller was proposed in ref[18], which converges the tracking error to an arbitrarily small polar limit and guarantees its transient performance with a preset maximum overshoot and convergence rate. A preset performance function describing the predefined trajectory tracking performance was designed to limit the rate of convergence, steady-state error, and maximum overshoot[19]. Using adaptive neural network control, the ultimate boundedness and predefined transient and steady-state performance of signals in the system are ensured. However, if input quantization is encountered during the controller design process, the aforementioned preset performance methods are no longer applicable. Underactuated unmanned surface ships are continuous systems, with control modules composed of digital processors. Quantization is a common process in digital signal transmission. These ships are networked systems, and their actual control signals must be converted from continuous to discrete to be transmitted to the next network. A quantizer is usually used in the conversion process to improve the sensor accuracy. In addition, it can save communication resources on the premise of ensuring performance. However,

the problems of strong nonlinearity and quantization errors occur during its usage, reducing the performance of the control system. To settle this problem, a fuzzy wavelet neural control method with improved preset performance was designed[20]. A hysteresis quantizer (HQ) has been added to the controller to avoid jitter without reducing control accuracy. A robust quantization control scheme is implemented to compensate for quantization errors. In ref[21], the challenge of realizing preset performance trajectory tracking control for underactuated underwater vehicles under the influence of complex Marine interference and input quantification is discussed. The constraint issue is transformed into an unconstrained problem through a mapping function, and a lag quantizer is added to effectively reduce the impact of quantization errors. Therefore, to achieve the closed-loop stability of unmanned surface ships after input quantization, addressing the compensation of the quantization error has become a problem worth paying attention to.

Inspired by the research results of the above article, this paper studies the matter of input quantization of the preset performance tracking control of underactuated unmanned surface ships based on the non-diagonal mass matrix and damping matrix model. It proposes an adaptive neural network control technology with guaranteed steady-state response and transient response tracking performance. Its main contributions can be summarized as follows:

(1) This article considers the dynamic models of the non-diagonal damping matrix and mass matrix of unmanned surface vessels, which can reflect a more realistic situation. To overcome unknown external environmental interference and model uncertainty, this paper designs an adaptive neural network tracking controller and uses an error transformation function to convert constrained tracking errors into unconstrained ones to ensure the specified preset performance;

(2) The control method proposed in this article can be used to consider input quantization constraints for unmanned vessel trajectory tracking tasks. In reality, in the process of controller design, if input quantization is encountered, the preset performance cannot be guaranteed. Therefore, we add a HQ to the controller to effectively reduce quantization errors while ensuring performance.

2.PROBLEM DESCRIPTION AND PRELIMINARY PREPARATION

2.1. Underactuated unmanned surface ship model
Assuming that the research object of this article is an underactuated unmanned surface ship with three degrees of freedom, its kinematics model is established as

$$\dot{\eta} = J(\eta) v \tag{1}$$

where $\eta = [x, y, \psi]^T$ denotes the position and attitude vector of the underactuated unmanned surface ship in the inertial frames; $v = [u, v, r]^T$ indicates the linear velocity and angular velocity vector of the underactuated unmanned surface ship in the hull coordinate system; $J(\eta)$ is the transform matrix between the two coordinate systems, expressed as

$$J(\eta) = \begin{bmatrix} \cos(\psi) & -\sin(\psi) & 0 \\ \sin(\psi) & \cos(\psi) & 0 \\ 0 & 0 & 1 \end{bmatrix}$$

The dynamics model of underactuated unmanned surface ships is denoted as

$$M\dot{v} + C(v)v + D(v)v = Q(\tau) + d \tag{2}$$

where M, $C(v)$, and $D(v)$ denote the mass matrix, Coriolis matrix, and linear hydrodynamic damping parameter matrix, respectively. $d=[d_1, d_2, d_3]^T$ is the unknown disturbance vector of the external environment.

$Q(\tau) = [Q(\tau_u), 0, Q(\tau_r)]^T$ is the quantization control input vector, where τ_u and τ_r are the longitudinal propulsion force and steering torque of the underactuated unmanned surface ship.

$C(v)$, $D(v)$, and M are given as

$$C(v) = \begin{bmatrix} 0 & 0 & c_{13} \\ 0 & 0 & c_{23} \\ c_{31} & c_{32} & 0 \end{bmatrix} = \begin{bmatrix} 0 & 0 & -m_{11}v - m_{23}r \\ 0 & 0 & m_{11}u \\ m_{11}v + m_{23}r & -m_{11}u & 0 \end{bmatrix}$$

$$D(v) = \begin{bmatrix} X_u & 0 & 0 \\ 0 & Y_v & Y_r \\ 0 & N_v & N_r \end{bmatrix} = \begin{bmatrix} d_{11} & 0 & 0 \\ 0 & d_{22} & d_{23} \\ 0 & d_{32} & d_{33} \end{bmatrix}$$

$$M = \begin{bmatrix} m_{11} & 0 & 0 \\ 0 & m_{22} & m_{23} \\ 0 & m_{32} & m_{33} \end{bmatrix} = \begin{bmatrix} -X_{\dot{u}} - m & 0 & 0 \\ 0 & -Y_{\dot{v}} - m & -Y_{\dot{v}} - mx_g \\ 0 & -N_{\dot{v}} - mx_g & -N_{\dot{r}} - I_z \end{bmatrix}$$

where m is the mass of the underactuated unmanned surface ship, I_z is the moment of inertia, and other parameter variables such as $X_{\dot{u}}$ are hydrodynamic derivatives. To convert the actual continuous signal into a discrete one, the following HQ is used [21]

$$Q(\tau_i) = \begin{cases} Q(\tau_i(t^-)), & \dot{\tau}_i = 0 \\ 0 & \frac{\tau_{i\min}}{1+\delta_i} < |\tau_i| \le \tau_{i\min}, \dot{\tau}_i > 0, or \quad 0 \le |\tau_i| < \frac{\tau_{i\min}}{1+\delta_i}, \dot{\tau}_i < 0 \\ \tau_{ir}(1+\delta_i)\,sign(\tau_i), & \frac{\tau_{ir}}{1-\delta_i} < |\tau_i| \le \frac{\tau_{ir}(1+\delta_i)}{1-\delta_i}, \dot{\tau}_i > 0, or \quad \tau_{ir} < |\tau_i| \le \frac{\tau_{ir}}{1-\delta_i}, \dot{\tau}_i < 0 \\ \tau_{ir}\,sign(\tau_i), & \tau_{ir} < |\tau_i| \le \frac{\tau_{ir}}{1-\delta_i}, \dot{\tau}_i > 0, or \quad \frac{\tau_{ir}}{1+\delta_i} < |\tau_i| < \tau_{ir}, \dot{\tau}_i < 0 \end{cases} \tag{3}$$

where $r = 1, 2, \ldots$, $i = u, r$, $\tau_{ir} = \rho^{1-r}\tau_{mi}$, and $\tau_{mi} > 0$, $\rho = \frac{1-\delta_i}{1+\delta_i}$, $\delta_i \in (01)$. $\tau_{i\min}$ is the minimum quantization level that determines the dead zone of $Q(\tau_i)$, $\rho \in (01)$ is the quantization density, and the larger ρ is, the higher the quantizer accuracy is. r is the quantization level, and $Q(\tau_i)$ is ultimately restricted to the set $U = \{0 \pm \tau_{ir}, \pm \tau_{ir}(1+\delta_i)\}$. A linear factorization of input quantization $Q(\tau_i)$ is proposed in ref[21], expressed as

$$Q(\tau_i) = \tau_i + \zeta_i \tag{4}$$

where $\zeta_i = Q(\tau_i) - \tau_i$ is the quantization error and satisfies Lemma 1.

Assumption 1 [22]. The expected trajectory (x_d, y_d, ψ_d) of an underactuated unmanned surface ship is smooth, and there are first-order and second-order differentials.

Assumption 2 [21]. The external disturbances d_1, d_2, and d_3 acting on the underactuated unmanned surface ship are time-varying disturbances and meet $|d_1| \le d_1^*$, $|d_2| \le d_2^*$, and $|d_3| \le d_3^*$, where $d_1^* > 0$, $d_2^* > 0$ and $d_3^* > 0$ indicate that the superior limit and bound value of the external disturbance are known.

Lemma 1 [23]. The quantization error ζ_i satisfies

$$\begin{cases} \zeta_i^2 \le \delta_i^2 \tau_i^2, & \forall |\tau_i| \ge \tau_{i\min} \\ \zeta_i^2 \le \tau_{i\min}^2, & \forall |\tau_i| \le \tau_{i\min} \end{cases} \tag{5}$$

In practical applications, the dynamic model of unmanned surface ships has parameter uncertainties, namely $M = M_0 + \Delta M$, $C = C_0 + \Delta C$, $D = D_0 + \Delta D$, where M_0, C_0, and D_0 are determinable parts and ΔM, ΔC, and ΔD are uncertain parts. Therefore, the dynamic model of unmanned surface ships can be denoted as

$$M_0 \dot{v} = -C_0(v)v - D_0(v)v + Q(\tau_i) - \Xi \tag{6}$$

where $\Xi = -\Delta M \dot{v} - \Delta C(v)v + d$.

Since the shape of most unmanned surface vessels is not always a semi-submerged sphere, and their mass matrix and damping matrix are non-diagonal, using coordinate changes [24], $\bar{x} = x + \varepsilon \cos \psi$, $\bar{y} = y + \varepsilon \sin \psi$, $\bar{v} = v + \varepsilon r$, $\varepsilon = m_{23}/m_{22}$, the nonlinear kinematics and dynamics equations of underactuated unmanned surface ships can be established as

$$\begin{cases} \dot{\bar{x}} = u \cos \psi - \bar{v} \sin \psi \\ \dot{\bar{y}} = u \sin \psi + \bar{v} \cos \psi \\ \dot{\psi} = r \\ \dot{u} = \left(m_{22} vr + m_{23} r^2 - d_{11} u + \Xi_u + Q(\tau_u) \right)/m_{11} \\ \dot{\bar{v}} = -(m_{11} ur + d_{22} v + d_{23} r - \Xi_v)/m_{22} \\ \dot{r} = (\phi + (-m_{23}\Xi_v + m_{22}\Xi_r) + m_{22}Q(\tau_r))/\left(m_{22}m_{33} - m_{23}^2\right) \end{cases} \tag{7}$$

where $\phi = \left(m_{11}m_{22} - m_{22}^2\right)uv + (m_{11}m_{23} - m_{22}m_{23})ur - m_{22}(d_{33}r + d_{32}v) + m_{23}(d_{23}r + d_{22}v)$.

Remark 1. In most neural network-based adaptive trajectory tracking control for underactuated unmanned surface ships, prior knowledge about the dynamics model of unmanned ships is not required. However, unlike traditional methods, this paper fully utilizes them to reduce the number of nodes and improve computational efficiency.

Remark 2. Due to the lack of driving devices on the lateral side of underactuated unmanned surface ships, only two control inputs, τ_u and τ_r, are considered in the dynamic model. The underactuated unmanned surface ship described by Equation (7) is underactuated and neglects roll motion. The trajectory tracking control of underactuated unmanned surface ships is more challenging than fully actuated ones.

Remark 3. In solving autonomous underwater vehicle tracking problems, better preset performance is achieved, but these methods cannot achieve preset performance when encountering input quantization. Therefore, in the tracking problem of underactuated unmanned surface vessels, achieving good preset performance while solving input quantization is the problem that needs to be implemented in the control method proposed in this article.

Remark 4. The real ship is not a semi-underwater sphere. Although the diagonal matrix is relatively easier to calculate in the system, in order to reflect the real situation, this article considers an unmanned surface ship model with a non-diagonal damping matrix and mass matrix.

2.2. Prescribed performance
In this article, the position errors of underactuated unmanned surface ships are defined as e_1 and e_2, and the heading Angle errors are represented by e_3. To achieve preset transient performance (i.e., overshoot and error convergence speed), the boundary function form is designed as

$$-\rho_i(t) < e_i(t) < \rho_i(t), i = 1, 2, 3 \tag{8}$$

where the performance function $\rho_i(t)$ is a design parameter and monotonically decreasing in the defined time domain, and $\lim_{t\to\infty}\rho_i(t) \to \rho_{i,\infty} > 0$, determined by

$$\rho_i(t) = (\rho_{i,0} - \rho_{i,\infty})\exp(-\kappa_i t) + \rho_{i,\infty} \tag{9}$$

where $\rho_{i,0}$, $\rho_{i,\infty}$, and κ_i are all positive real numbers, and κ_i indicates the lower limit of interest rate at which the tracking error converges. To achieve the preset tracking performance, we then convert the above inequality constraint Equation (8) into an equality constraint

$$e_i^* = \Upsilon(z_i) = \ln\left(\frac{1 + z_i}{1 - z_i}\right) \tag{10}$$

where $z_i = \frac{e_i}{\rho_i}$, and $\Upsilon(.)$ are smooth functions with bijection and strictly monotonically increasing, and $\Upsilon(.) \to (-\infty, \infty)$, $\Upsilon(0) = 0$.

Lemma 2 [25]. If the position error and yaw angle errors e_1, e_2, and e_3 and transform errors e_1^*, e_2^*, and e_3^* are bounded, then the preset performance can be achieved.

2.3. Radial basis function neural networks

In control, the RBFNN has a relatively uncomplicated structure and universal approximation property, which provides an effective solution for solving nonlinear control problems. In this article, we use the traditional RBFNN control algorithm to approximate the uncertain fluid dynamics and the unknown disturbance sum $f(Z)$. The output expression of the neural network for the unknown part $f(Z)$ is established as

$$f(Z) = \xi(Z) + S(Z)W^{*T} \forall Z \in \Omega \tag{11}$$

where Z is the input vector of the RBFNN, and $\xi(Z)$ is the bounded approximation error of the neural network and satisfies $\xi(Z) \le \xi^*$; $S(Z) = [S_1(x), S_2(x), \cdots, S_n(x)]^T$ is the regression vector, and the output expression of the basis function is denoted as

$$S_i(Z) = \exp\left[-\frac{(Z - c_i)^T(Z - c_i)}{\sigma_i^2}\right], i = 1, 2, \cdots, n \tag{12}$$

where the input vector Z and the vector value c_i of the center point of the Gaussian basis function have the same dimension, and σ_i is the radial basis function width.

$W^* = [w_1^*, w_2^*, \cdots, w_n^*]^T$ denotes the optimal neural network weight vector, defined as

$$W^* = \arg\min_{W^* \in R^n}\left[\sup_{Z \in \Omega}\left|f(Z) - \hat{W}^T S(Z)\right|\right] \tag{13}$$

where $\hat{W}$ is the estimate of W^*. Assuming that the weight W^* of the neural network is bounded; i.e., there exists a constant W greater than zero, such that $\|W^*\| \le W$.

2.4. Trajectory tracking problem

In this paper, $\eta = [x, y, \psi]^T$ is the practical position of the underactuated unmanned surface ship, and $\eta_d = [x_d, y_d, \psi_d]^T$ is the given reference trajectory. Define the trajectory tracking error as

$$\begin{cases} e_1 = \bar{x} - \bar{x}_d \\ e_2 = \bar{y} - \bar{y}_d \\ e_3 = \psi - \psi_a \end{cases} \tag{14}$$

where $\bar{x}_d = x_d + \varepsilon\cos\psi_d, \bar{y}_d = y_d + \varepsilon\sin\psi_d$. ψ_a is an angle related to e_1, e_2, and e_3, defined as [22]

$$\psi_a = \beta\tanh\left(H^2/a_1\right) + \psi_d\left(1 - \tanh\left(H^2/a_1\right)\right) \tag{15}$$

where a_1 is a normal number, and $\beta = \tan^{-1}\left(\frac{-e_2}{-e_1}\right)$ and $H = \sqrt{e_1^2 + e_2^2}$.

3. TRAJECTORY TRACKING CONTROLLER DESIGN

In this chapter, an adaptive trajectory tracking controller for underactuated unmanned surface ships is designed based on neural networks. Firstly, an appropriate virtual control law is designed; then, the derivative of transformation error $e_i^*(i = 1, 2, 3)$ is derived, and finally, the derivative of velocity error $s_i(i = 1, 2, 3)$ is derived, and the τ_u and τ_r are designed. Derivation of both sides of the ship trajectory tracking error Equation (14) concerning time t can be obtained as

$$
\begin{bmatrix} \dot{e}_1 \\ \dot{e}_2 \\ \dot{e}_3 \end{bmatrix} = \begin{bmatrix} \cos\psi & -\sin\psi & 0 \\ \sin\psi & \cos\psi & 0 \\ 0 & 0 & 1 \end{bmatrix} \begin{bmatrix} u \\ \bar{v} \\ r \end{bmatrix} - \begin{bmatrix} \dot{\bar{x}}_d \\ \dot{\bar{y}}_d \\ \dot{\psi}_d \end{bmatrix} \tag{16}
$$

where u, $\bar{v}$, and r are regarded as practical control quantities. To realize the trajectory tracking position error $e_i^*(i = 1, 2, 3)$ after the transformation of unmanned surface ships tends to zero under the preset performance, the virtual control law is specifically designed as

$$
\begin{bmatrix} \alpha_u \\ \alpha_v \\ \alpha_r \end{bmatrix} = \begin{bmatrix} \cos\psi & \sin\psi & 0 \\ -\sin\psi & \cos\psi & 0 \\ 0 & 0 & 1 \end{bmatrix} \begin{bmatrix} \dot{\bar{x}}_d - l_1 e_1^* \\ \dot{\bar{y}}_d - l_1 e_2^* \\ \dot{\psi}_d - l_2 e_3^* \end{bmatrix} \tag{17}
$$

where $l_1 > 0$ and $l_2 > 0$ are design constants.

$$
\begin{bmatrix} \dot{e}_1 \\ \dot{e}_2 \\ \dot{e}_3 \end{bmatrix} = \begin{bmatrix} -l_1 \dot{e}_1^* \\ -l_1 \dot{e}_2^* \\ -l_2 \dot{e}_3^* \end{bmatrix} + \begin{bmatrix} \cos\psi & -\sin\psi & 0 \\ \sin\psi & \cos\psi & 0 \\ 0 & 0 & 1 \end{bmatrix} \begin{bmatrix} u - \alpha_u \\ \bar{v} - \alpha_v \\ r - \alpha_r \end{bmatrix} \tag{18}
$$

According to [25], the speed error is defined as

$$
\begin{aligned}
u_e &= u - \alpha_u \\
v_e &= \bar{v} - \alpha_v - \beta_2 \tanh\gamma_2 \\
r_e &= r - \alpha_r
\end{aligned} \tag{19}
$$

where β_2 is a design parameter, $\alpha = [\alpha_u \alpha_v \alpha_r]^T$ is a virtual control quantity, and γ_2 is used to deal with the underdrive problem of underactuated unmanned surface ships. Substituting Equation (19) into (18) yields

$$
\begin{bmatrix} \dot{e}_1 \\ \dot{e}_2 \\ \dot{e}_3 \end{bmatrix} = \begin{bmatrix} -l_1 \dot{e}_1^* \\ -l_1 \dot{e}_2^* \\ -l_2 \dot{e}_3^* \end{bmatrix} + \begin{bmatrix} \cos\psi & -\sin\psi & 0 \\ \sin\psi & \cos\psi & 0 \\ 0 & 0 & 1 \end{bmatrix} \begin{bmatrix} u_e + \alpha_u \\ \bar{v}_e + \alpha_v + \beta_2 \tanh\gamma_2 \\ r_e + \alpha_r \end{bmatrix} \tag{20}
$$

Construct the following Lyapunov function

$$
V = V_1 + V_2 \tag{21}
$$

where

$$
V_1 = \frac{1}{2} \left(f_1 e_1^{*2} + f_2 e_2^{*2} + f_3 e_3^{*2} \right) \tag{22}
$$

By differentiating Equation (22), we can get

$$
\dot{V}_1 = f_1 e_1^* \dot{e}_1^* + f_2 e_2^* \dot{e}_2^* + f_3 e_3^* \dot{e}_3^* \tag{23}
$$

By differentiating the Equation (10), we get

$$
\dot{e}_i^* = \frac{2 \left(\rho_i \dot{e}_i - e_i \dot{\rho}_i \right)}{\left(1 - z_i^2 \right) \rho_i^2}, i = 1, 2, 3 \tag{24}
$$

Substituting the Equation (20) into the above equation can obtain

$$
\begin{aligned}
\dot{e}_1^* &= \frac{2\left(-l_1 e_1^* + u_e \cos\psi - v_e \sin\psi + \iota_1\right)}{\left(1 - z_1^2\right)\rho_1} \\
\dot{e}_2^* &= \frac{2\left(-l_1 e_2^* + u_e \sin\psi + v_e \cos\psi + \iota_2\right)}{\left(1 - z_2^2\right)\rho_2} \\
\dot{e}_3^* &= \frac{2\left(-l_2 e_3^* + r_e + \iota_3\right)}{\left(1 - z_3^2\right)\rho_3}
\end{aligned}
\tag{25}
$$

where $f_i = \left(1 - z_i^2\right)\rho_i$, $\iota_1 = -\alpha_2 \tanh\beta_2 \sin\psi + \dot{\rho}_1 z_1$, $\iota_2 = \alpha_2 \tanh\beta_2 \cos\psi - \dot{\rho}_2 z_2$, and $\iota_3 = \dot{\psi}_d - \dot{\rho}_3 z_3$. Substituting Equation (25) into Equation (23) can get

$$
\begin{aligned}
\dot{V}_1 \leq{}& -2l_1 e_1^{*2} - 2l_1 e_2^{*2} - 2l_2 e_3^{*2} + 2\left|e_1^* u_e\right| + 2\left|e_1^* v_e\right| + 2\left|e_2^* u_e\right| + 2\left|e_2^* v_e\right| + 2\left|e_3^* r_e\right| \\
&+ 2e_1^* \iota_1 + 2e_2^* \iota_2 + 2e_3^* \iota_3 - 2\left(l_1 - 1\right)e_1^{*2} - 2\left(l_1 - 1\right)e_2^{*2} - 2\left(l_2 - 1\right)e_3^{*2} \\
&+ 2(u_e^2 + v_e^2 + r_e^2) + \sum_{i=1}^{3} \bar{\iota}_i^2
\end{aligned}
\tag{26}
$$

Using Young's inequality, Equation (26) can be written as

$$
\begin{aligned}
\dot{V}_1 \leq{}& -2l_1 e_1^{*2} - 2l_1 e_2^{*2} - 2l_2 e_3^{*2} + 2\left|e_1^* u_e\right| + 2\left|e_1^* v_e\right| + 2\left|e_2^* u_e\right| + 2\left|e_2^* v_e\right| + 2\left|e_3^* r_e\right| \\
&+ 2e_1^* \iota_1 + 2e_2^* \iota_2 + 2e_3^* \iota_3 - 2\left(l_1 - 1\right)e_1^{*2} - 2\left(l_1 - 1\right)e_2^{*2} - 2\left(l_2 - 1\right)e_3^{*2} \\
&+ 2(u_e^2 + v_e^2 + r_e^2) + \sum_{i=1}^{3} \bar{\iota}_i^2
\end{aligned}
\tag{27}
$$

Remark 4. If the position error and yaw angle error e_1, e_2, and e_3 transform errors e_1^*, e_2^*, and e_3^* are bounded, then the preset performance can be achieved.

According to Equations (8) and (10), we know that $|z_i| \leq 1$, $|\rho_i| \leq \alpha_i \left(\rho_{i,0} - \rho_{i,\infty}\right)$, $i = 1, 2, 3$, so there is a positive constant $\bar{\iota}_i \geq \iota_i$.

Derivation of Equation (19) concerning time is obtained as

$$
\begin{aligned}
\dot{u}_e &= \phi_u + d_u + Q\left(\tau_u\right)/m_{11} - \dot{\alpha}_u \\
\dot{v}_e &= \phi_v + d_v - \beta_2 \dot{\gamma}_2 \operatorname{sech}^2\gamma_2 - \dot{\alpha}_v \\
\dot{r}_e &= \phi_r + d_r + m_{22} Q\left(\tau_r\right)/\Delta - \dot{\alpha}_r
\end{aligned}
\tag{28}
$$

where $\phi_u = \left(m_{22} vr + m_{23} r^2 - d_{11} u\right)/m_{11}$, $\phi_v = -(m_{11} ur + d_{22} v + d_{23} r)/m_{22}$, $\phi_r = \left\{\left(m_{11} m_{22} - m_{22}^2\right) uv + \left(m_{11} m_{23} - m_{22} m_{23}\right) ur - m_{22}\left(d_{33} r + d_{32} v\right) + m_{23}\left(d_{23} r + d_{22} v\right)\right\}/\Delta$, $\Delta = m_{22} m_{33} - m_{23}^2$, $d_u = \Xi_u/m_{11}$, $d_v = \Xi_v/m_{22}$, and $d_r = \left(-m_{23}\Xi_v + m_{22}\Xi_r\right)/\Delta$. refFurthermore, γ_2 is given by

$$
\dot{\gamma}_2 = \cosh^2\gamma_2\left(\hat{W}_v^T S_v\left(Z\right) + \phi_v - l_3 u_e + l_3 v_e - l_3 r_e\right)/\beta_2
\tag{29}
$$

By plugging the Equation (29) into the Equation (28), we can get

$$
\begin{aligned}
\dot{u}_e &= \phi_u + d_u + Q\left(\tau_u\right)/m_{11} - \dot{\alpha}_u \\
\dot{v}_e &= d_v + l_3 u_e - l_3 v_e + l_3 r_e - \hat{W}_v^T S_v\left(Z\right) - \dot{\alpha}_v \\
\dot{r}_e &= \phi_r + d_r + m_{22} Q\left(\tau_r\right)/\Delta - \dot{\alpha}_r
\end{aligned}
\tag{30}
$$

We define $W_u^{*T} S_u (Z) + \xi_1 = d_u - \dot{\alpha}_u$, $W_v^{*T} S_v (Z) + \xi_2 = d_v - \dot{\alpha}_v$, $W_r^{*T} S_r (Z) + \xi_3 = d_r - \dot{\alpha}_r$, and the Equation (30) can be rewritten as

$$
\begin{aligned}
\dot{u}_e &= \phi_u + Q(\tau_u)/m_{11} + W_u^{*T} S_u (Z) + \xi_1 \\
\dot{v}_e &= l_3 u_e - l_3 v_e + l_3 r_e - \tilde{W}_v^T S_v (Z) + \xi_2 \\
\dot{r}_e &= \phi_r + m_{22} Q(\tau_r)/\Delta + W_r^{*T} S_r (Z) + \xi_3
\end{aligned}
\tag{31}
$$

where $Z = \begin{bmatrix} u & v & r & \alpha_u & \alpha_v & \alpha_r & e_1^* & e_2^* & e_3^* \end{bmatrix}^T$ is the input vector of the neural network. Select the Lyapunov function

$$
V_2 = \frac{1}{2} \left(u_e^2 + v_e^2 + r_e^2 \right) + \frac{1}{2\Gamma_u} \tilde{W}_u^T \tilde{W}_u + \frac{1}{2\Gamma_v} \tilde{W}_v^T \tilde{W}_v + \frac{1}{2\Gamma_r} \tilde{W}_r^T \tilde{W}_r
\tag{32}
$$

With the help of Equation (32), derivation of Equation (33) concerning time can be obtained as

$$
\begin{aligned}
\dot{V}_2 &= u_e \dot{u}_e + v_e \dot{v}_e + r_e \dot{r}_e + \frac{1}{\Gamma_u} \tilde{W}_u^T \dot{\hat{W}}_u + \frac{1}{\Gamma_v} \tilde{W}_v^T \dot{\hat{W}}_v + \frac{1}{\Gamma_r} \tilde{W}_r^T \dot{\hat{W}}_r \\
&= u_e \left(\phi_u + (\tau_u + \zeta_u)/m_{11} + W_u^{*T} S_u (Z) + \xi_1 \right) \\
&\quad + v_e \left(l_3 u_e - l_3 v_e + l_3 r_e - \tilde{W}_v^T S_v (Z) + \xi_2 \right) \\
&\quad + r_e \left(\phi_r + m_{22} (\tau_r + \zeta_r)/\Delta + W_r^{*T} S_r (Z) + \xi_3 \right) \\
&\quad + \frac{1}{\Gamma_u} \tilde{W}_u^T \dot{\hat{W}}_u + \frac{1}{\Gamma_v} \tilde{W}_v^T \dot{\hat{W}}_v + \frac{1}{\Gamma_r} \tilde{W}_r^T \dot{\hat{W}}_r
\end{aligned}
\tag{33}
$$

Design an auxiliary control signal generator as

$$
\begin{cases}
\gamma_1 = k_1 u_e + \phi_u + \hat{W}_u^T S_u (Z) + l_3 u_e + l_3 v_e \\
\gamma_3 = k_3 r_e + \phi_r + \hat{W}_r^T S_r (Z) + l_3 v_e + l_3 r_e
\end{cases}
\tag{34}
$$

where k_1 and k_3 are the controller gains of the speed subsystem. Compensating for quantization errors, $u_e \gamma_u$ and $r_e \gamma_r$ are added to Equation (34), and then $u_e \gamma_u$ and $r_e \gamma_r$ are subtracted. Then, Equation (34) can be rewritten as

$$
\begin{aligned}
\dot{V}_2 &= \left((\zeta_u + \tau_u)/m_{11} + \phi_u + W_u^{*T} S_u (Z) + \xi_1 \right) u_e + \gamma_u u_e - \gamma_u u_e \\
&\quad + v_e \left(l_3 u_e - l_3 v_e + l_3 r_e - \tilde{W}_v^T S_v (Z) + \xi_2 \right) \\
&\quad + \left(\phi_r + m_{22} (\zeta_r + \tau_r)/\Delta + W_r^{*T} S_r (Z) + \xi_3 \right) r_e + r_e \gamma_r - r_e \gamma_r \\
&\quad + \frac{1}{\Gamma_u} \tilde{W}_u^T \dot{\hat{W}}_u + \frac{1}{\Gamma_v} \tilde{W}_v^T \dot{\hat{W}}_v + \frac{1}{\Gamma_r} \tilde{W}_r^T \dot{\hat{W}}_r
\end{aligned}
\tag{35}
$$

By substituting Equation (34) into Equation (35), we can get

$$
\begin{aligned}
\dot{V}_2 &= u_e \gamma_u + u_e \left((\tau_u + \zeta_u)/m_{11} - \tilde{W}_u^T S_u (Z) + \xi_1 - l_3 u_e - k_1 u_e \right) \\
&\quad + v_e \left(-l_3 v_e - \tilde{W}_v^T S_v (Z) + \xi_2 \right) \\
&\quad + r_e \gamma_r + r_e \left(m_{22} (\tau_r + \zeta_r)/\Delta - \tilde{W}_r^T S_r (Z) + \xi_3 - l_3 r_e - k_3 r_e \right) \\
&\quad + \tilde{W}_u^T \left(S_u (Z) u_e - \vartheta_u \hat{W}_u \right) + \tilde{W}_v^T \left(S_v (Z) v_e - \vartheta_v \hat{W}_v \right) + \tilde{W}_r^T \left(S_r (Z) r_e - \vartheta_r \hat{W}_r \right) \\
&= u_e \gamma_u + u_e (\tau_u + \zeta_u)/m_{11} + r_e \gamma_r + r_e m_{22} (\tau_r + \zeta_r)/\Delta \\
&\quad - l_3 u_e^2 - k_1 u_e^2 - l_3 v_e^2 - l_3 r_e^2 - k_3 r_e^2 + \xi_1 u_e + \xi_2 v_e + \xi_3 r \\
&\quad - \tilde{W}_u^T \vartheta_u \hat{W}_u - \tilde{W}_v^T \vartheta_v \hat{W}_v - \tilde{W}_r^T \vartheta_r \hat{W}_r
\end{aligned}
\tag{36}
$$

where $\tilde{W}_i = W_i^* - \hat{W}_i$ represents the weight estimation error. Design practical control method and weight adaptive law as

$$\tau_u = -\frac{m_{11} u_e \gamma_1^2}{(1 - \delta_1) \sqrt{u_e^2 \gamma_1^2 + \beta_1^2}}$$

$$\tau_r = -\frac{\Delta r_e \gamma_3^2}{m_{22} (1 - \delta_3) \sqrt{r_e^2 \gamma_3^2 + \beta_3^2}} \tag{37}$$

$$\dot{\hat{W}}_i = \Gamma_i \left(i_e S_i (Z) - \vartheta_i \hat{W}_i \right), i = u, v, r$$

where $\vartheta_i > 0$, β_1, and β_3 are the design parameters, and $\beta_1 > 0$, $\beta_3 > 0$. According to the Young's inequality, one has

$$\tau_{u \min} |u_e| \leq \frac{1}{4} \tau_{u \min}^2 + u_e^2$$

$$\tau_{r \min} |r_e| \leq \frac{1}{4} \tau_{r \min}^2 + r_e^2 \tag{38}$$

where $0 < \delta_1 < 1$, $0 < \delta_3 < 1$, and $u_e \tau_u < 0$, $r_e \tau_r < 0$. According to Lemma 1, we can obtain

$$\zeta_u \leq \delta_i |u_e| + \tau_{u \min}$$

$$\zeta_r \leq \delta_i |r_e| + \tau_{r \min} \tag{39}$$

According to Equations (39) and (40), we can obtain

$$\begin{aligned}
\frac{(\zeta_u + \tau_u) u_e}{m_{11}} &= \frac{\zeta_u u_e}{m_{11}} + \frac{\tau_u u_e}{m_{11}} \\
&\leq \frac{|\tau_u u_e| \delta_1}{m_{11}} + \frac{\tau_u u_e}{m_{11}} + \frac{\tau_{u \min} |u_e|}{m_{11}} \\
&\leq \frac{(1 - \delta_1) u_e \tau_u}{m_{11}} + \frac{u_e^2}{m_{11}} + \frac{\tau_{u \min}^2}{4 m_{11}} \\
&\leq -\frac{u_e^2 \gamma_u^2}{\sqrt{u_e^2 \gamma_u^2 + \beta_1^2}} + \frac{u_e^2}{m_{11}} + \frac{\tau_{u \min}^2}{4 m_{11}}
\end{aligned} \tag{40}$$

Consider

$$-\frac{u_e^2 \gamma_u^2}{\sqrt{u_e^2 \gamma_u^2 + \beta_1^2}} \leq -\frac{(u_e \gamma_u)^2}{|u_e \gamma_u| + \beta_1} < -\frac{(u_e \gamma_u)^2 + \beta_1^2}{|u_e \gamma_u| + \beta_1} \leq \beta_1 - u_e \gamma_u \tag{41}$$

Thus

$$\frac{(\zeta_u + \tau_u) u_e}{m_{11}} \leq \beta_1 - u_e \gamma_e + \frac{u_e^2}{m_{11}} + \frac{\tau_{u \min}^2}{4 m_{11}} \tag{42}$$

Similarly, there are

$$\frac{m_{22} r_e (\tau_r + \zeta_r)}{\Delta} \leq \beta_3 - r_e \gamma_r + \frac{m_{22} r_e^2}{\Delta} + \frac{m_{22} \tau_{r \min}^2}{4 \Delta} \tag{43}$$

Substituting Equations (42) and (43) into Equation (36), we have

$$
\begin{aligned}
\dot{V}_2 \leq\ & u_e \gamma_u + \beta_1 - u_e \gamma_u + \frac{u_e^2}{m_{11}} + \frac{\tau_{u\,\min}^2}{4m_{11}} \\
& + r_e \gamma_r + \beta_3 - r_e \gamma_r + \frac{m_{22} r_e^2}{\Delta} + \frac{m_{22} \tau_{r\,\min}^2}{4\Delta} \\
& - l_3 u_e^2 - k_1 u_e^2 - l_3 v_e^2 - l_3 r_e^2 - k_3 r_e^2 + \xi_1 u_e + \xi_2 v_e + \xi_3 r \\
& - \tilde{W}_u^T \vartheta_u \hat{W}_u - \tilde{W}_v^T \vartheta_v \hat{W}_v - \tilde{W}_r^T \vartheta_r \hat{W}_r \\
=\ & -\left(-\frac{1}{m_{11}} + l_3 + k_1\right) u_e^2 - l_3 v_e^2 - \left(-\frac{m_{22}}{\Delta} + l_3 + k_3\right) r_e^2 \\
& + \xi_1 u_e + \xi_2 v_e + \xi_3 r + \beta_1 + \frac{\tau_{u\,\min}^2}{4m_{11}} + \beta_3 + \frac{m_{22} \tau_{r\,\min}^2}{4\Delta} \\
& - \tilde{W}_u^T \vartheta_u \hat{W}_u - \tilde{W}_v^T \vartheta_v \hat{W}_v - \tilde{W}_r^T \vartheta_r \hat{W}_r
\end{aligned}
\tag{44}
$$

Consider

$$
\begin{aligned}
\xi_1 u_e &\leq \frac{1}{2}\left(u_e^2 + \xi_1^2\right) \\
\xi_2 v_e &\leq \frac{1}{2}\left(v_e^2 + \xi_2^2\right) \\
\xi_3 r_e &\leq \frac{1}{2}\left(r_e^2 + \xi_3^2\right)
\end{aligned}
\tag{45}
$$

and

$$
\begin{aligned}
-\tilde{W}_i^T \vartheta_i \hat{W}_i &= -\tilde{W}_i^T \vartheta_i \left(\tilde{W}_i + W_i^*\right) \\
&\leq -\tilde{W}_i^T \vartheta_i \tilde{W}_i + \frac{\vartheta_i}{2} \tilde{W}_i^T \tilde{W}_i + \frac{\vartheta_i}{2} \left\|W_i^*\right\|^2 \\
&\leq -\frac{\vartheta_i}{2} \tilde{W}_i^T \tilde{W}_i + \frac{\vartheta_i}{2} \left\|W_i^*\right\|^2 \\
&\leq -\frac{\vartheta_i}{2} \tilde{W}_i^T \tilde{W}_i + \frac{\vartheta_i}{2} W_i^2
\end{aligned}
\tag{46}
$$

Substituting Equations (45) and (46) into $\dot{V}_2$, we have

$$
\begin{aligned}
\dot{V}_2 \leq\ & -\left(-\frac{1}{m_{11}} + l_3 + k_1 - \frac{1}{2}\right) u_e^2 - l_3 - \frac{1}{2} v_e^2 - \left(-\frac{m_{22}}{\Delta} + l_3 + k_3 - \frac{1}{2}\right) r_e^2 \\
& + \frac{\xi_1^2}{2} + \frac{\xi_2^2}{2} + \frac{\xi_3^2}{2} + \beta_1 + \frac{\tau_{u\,\min}^2}{4m_{11}} + \beta_3 + \frac{m_{22} \tau_{r\,\min}^2}{4\Delta} \\
& - \frac{\vartheta_u}{2} \tilde{W}_u^T \tilde{W}_u - \frac{\vartheta_v}{2} \tilde{W}_v^T \tilde{W}_v - \frac{\vartheta_r}{2} \tilde{W}_r^T \tilde{W}_r + \frac{\vartheta_u}{2} W_u^2 + \frac{\vartheta_v}{2} W_v^2 + \frac{\vartheta_r}{2} W_r^2
\end{aligned}
\tag{47}
$$

Substituting Equations (27) and (47) into Equation (21) yields:

$$
\begin{aligned}
\dot{V} \leq\ & -2(l_1 - 1) e_1^{*2} - 2(l_1 - 1) e_2^{*2} - 2(l_2 - 1) e_3^{*2} \\
& - \left(-\frac{1}{m_{11}} + l_3 + k_1 - \frac{5}{2}\right) u_e^2 - l_3 - \frac{5}{2} v_e^2 - \left(-\frac{m_{22}}{\Delta} + l_3 + k_3 - \frac{5}{2}\right) r_e^2 \\
& + \frac{\xi_1^2}{2} + \frac{\xi_2^2}{2} + \frac{\xi_3^2}{2} + \beta_1 + \frac{\tau_{u\,\min}^2}{4m_{11}} + \beta_3 + \frac{m_{22} \tau_{r\,\min}^2}{4\Delta} + \sum_{i=1}^{3} \tilde{\iota}_i^2 \\
& - \frac{\vartheta_u}{2} \tilde{W}_u^T \tilde{W}_u - \frac{\vartheta_v}{2} \tilde{W}_v^T \tilde{W}_v - \frac{\vartheta_r}{2} \tilde{W}_r^T \tilde{W}_r + \frac{\vartheta_u}{2} W_u^2 + \frac{\vartheta_v}{2} W_v^2 + \frac{\vartheta_r}{2} W_r^2 \\
\leq\ & -\mu V + C
\end{aligned}
\tag{48}
$$

where

$$\mu = \min\left(\frac{1}{m_{11}}, \frac{m_{22}}{\Delta}, k_1, k_3, l_3, \frac{\zeta_i}{2}, \vartheta_u, \vartheta_v, \vartheta_r\right)$$

$$C = \frac{\xi_1^2}{2} + \frac{\xi_2^2}{2} + \frac{\xi_3^2}{2} + \beta_1 + \frac{\tau_{u\,\min}^2}{4m_{11}} + \beta_3 + \frac{m_{22}\tau_{r\,\min}^2}{4\Delta} + \frac{\vartheta_u}{2}W_u^2 + \frac{\vartheta_v}{2}W_v^2 + \frac{\vartheta_r}{2}W_r^2 + \sum_{i=1}^{3}\tilde{\iota}_i^2$$

(49)

And then, Equation (47) can be transformed as

$$V(t) \le \left(-\frac{C}{\mu} + V(0)\right)e^{-\mu t} + \frac{C}{\mu}$$

(50)

where $V_2(t)$ converges when the center of the sphere with radius $\frac{C}{\mu}$ is in the sphere domain of the origin; that is, $V_2(t)$ is uniformly and finally bounded. Equation (48) indicates that signals $u_e, v_e, r_e, \tilde{W}_u, \tilde{W}_v$ and $\tilde{W}_r$ in the system are uniformly and ultimately bounded, and then from Equation (32) to Equation (48), the position tracking error $e_i^*(i = 1, 2, 3)$ of the surface unmanned ship is bounded, thus obtaining the consistent and ultimately bounded property of all error signals in the tracking control closed-loop system of underactuated unmanned surface ships.

4. SIMULATION ANALYSIS

To demonstrate the effectiveness of the control method proposed in this article, the underactuated unmanned surface vessel in the literature [24] was used as the simulation object for verification. Relevant parameters of underactuated unmanned surface ships are: $m_{11} = 141.85$, $d_{11} = u^2 \cdot 10 + 67.26|u| + 45.6$, $d_{22} = |r| \cdot 15 + |v| \cdot 73.85 + 29.54$, $m_{33} = 15.6 d_{23} = |r| \cdot 10.71 + |v| \cdot 2 - 2.5$, $d_{32} = -|r| \cdot 0.2 - |v| \cdot 13 - 2.4$, $c_{13} = -r \cdot 5.7 - v \cdot 191.75 d_{33} = -|r| \cdot 0.07 + |r| \cdot 10.71 + 5.59$, $c_{23} = u \cdot 141.85$, $m_{22} = 191.75$, $c_{31} = r \cdot 5.7 + v \cdot 191.75$, and $c_{32} = -u \cdot 141.85$. The forces and moments generated by unknown environmental disturbances are: $d_1 = 10^4 \cdot \cos(0.5t) + 10^4 \cdot \sin(0.3t)$, $d_2 = 10^2 \cdot \cos(0.4t) + 10^2 \cdot \sin(0.2t)$, and $d_3 = 10^5 \cdot \cos(0.2t) + 10^5 \cdot \sin(0.5t)$. The uncertainty of the model can be set to $\Delta(\eta, v) = [0.6, 0.2u^2, \sin(v) + 0.15r^2]^T$. Set the expected trajectory to $u_d = 0.6$, $v_d = 0 r_d = 0 0 \le t < 110$; $u_d = 0.6$, $v_d = 0$, $r_d = -0.006\sin(\pi(t - 100)/500) t \ge 110$. Select the initial state of the unmanned surface ship as $\eta_0 = (2, -3, 0)^T$, $v_0 = (0, 0, 0)^T$. The control parameter is $l_1 = 1$, $l_2 = 2$, $l_3 = 1$, $k_1 = 3$, $k_2 = 5$, $k_3 = 10$, $\vartheta_u = 1 \times 10^{-8}$, $\vartheta_v = 1 \times 10^{-5}$, $\vartheta_r = 1 \times 10^{-7}$, $\Gamma_1 = 1 \times 10^5$, $\Gamma_2 = 1 \times 10^4$, $\Gamma_3 = 1 \times 10^3$. In this paper, neural networks are used to approximate external environmental disturbances and model uncertainties, with a hidden layer node count of 39. The center points are evenly distributed over [-16,16], and the width of the Gaussian basis function is $\sigma_1 = 0.7 \times 10^{-8}$, $\sigma_3 = 1.5 \times 10^{-7}$. The initial value of the estimated weight is $\hat{W}_i = [0, 0, \ldots, 0]^T$, $i = u, r$. Predefined bounded functions are set to $\rho_1 = (18 - 2)e^{-0.05t} + 2$, $\rho_2 = (18 - 2)e^{-0.05t} + 2$, $\rho_3 = (3 - \frac{\pi}{6})e^{-0.05t} + \frac{\pi}{6}$. The parameter selection for the quantizer is $\sigma_u = 0.3$, $\sigma_v = 0.15$, $\tau_{u\,\min} = 0.003$, $\tau_{r\,\min} = 0.002$. The results of simulation verification are shown in Figures 1-7.

Figure 1 displays that the unmanned surface ship tracks the linear and curved reference trajectories in the case of unknown interference from the external environment and uncertainties in the model. The course of the unmanned surface ship changes from time to time when tracking the curve reference trajectories. Figures 2-4 demonstrate the tracking errors of the position and yaw angle of the underactuated unmanned surface ship. It can be seen that the position tracking error and yaw angle tracking error both meet preset constraints, and the tracking error of traditional Proportional-Integral (PI) controllers will violate the preset constraints. The tracking error of the controller will converge to approximately zero. Figures 5 and 6 exhibit the transformation from continuous signals to discrete signals of longitudinal control force and yawing control torque of an underactuated unmanned surface ship. The theorem of asymptotic convergence of quantization error is shown in the actual simulated relationship between τ_u, τ_r and $Q(\tau_u), Q(\tau_r)$. This is the key to ensuring the stability of quantitative control. Figure 7 illustrates the neural weight norm.
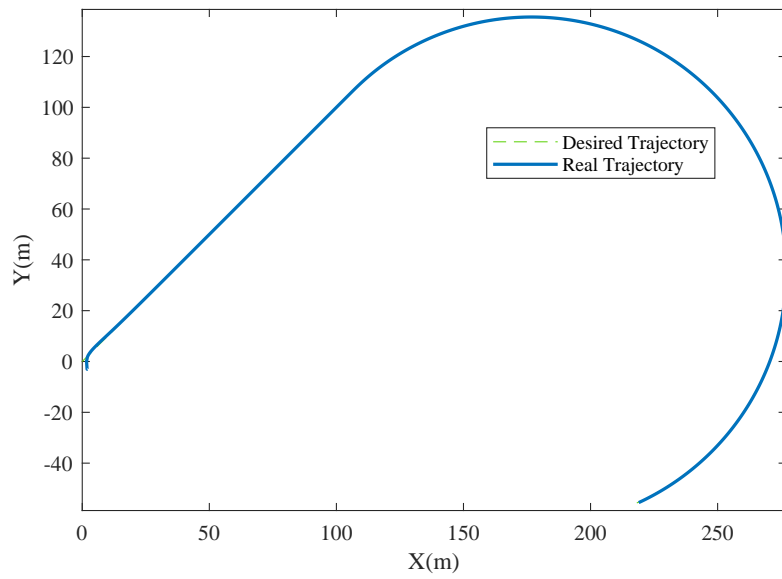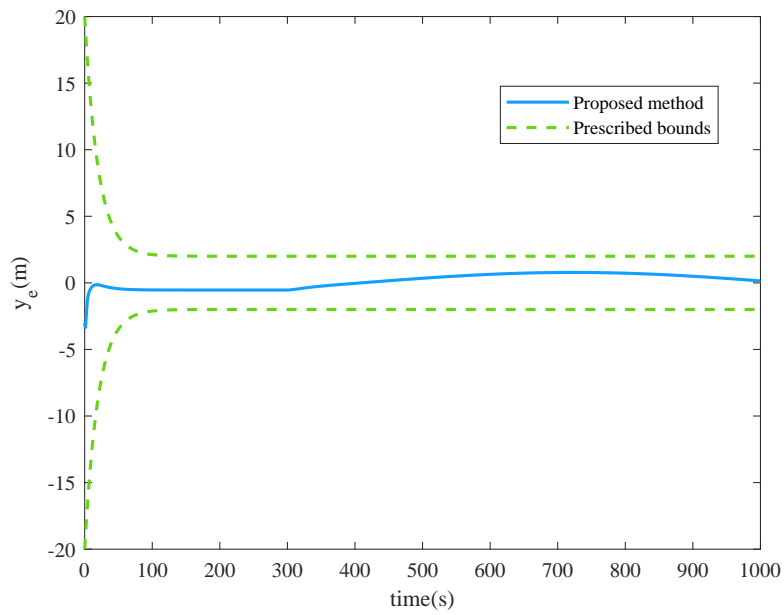
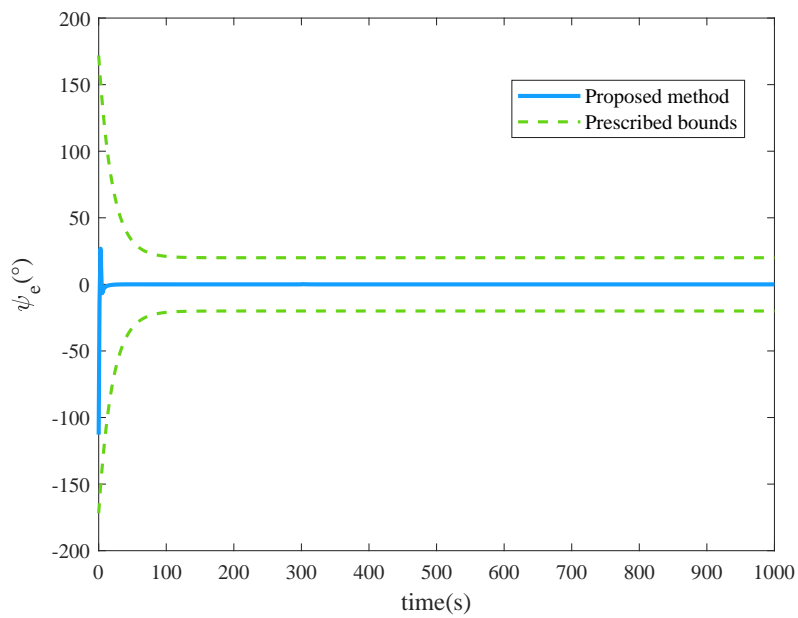**Figure 1.** Trajectory tracking curve.
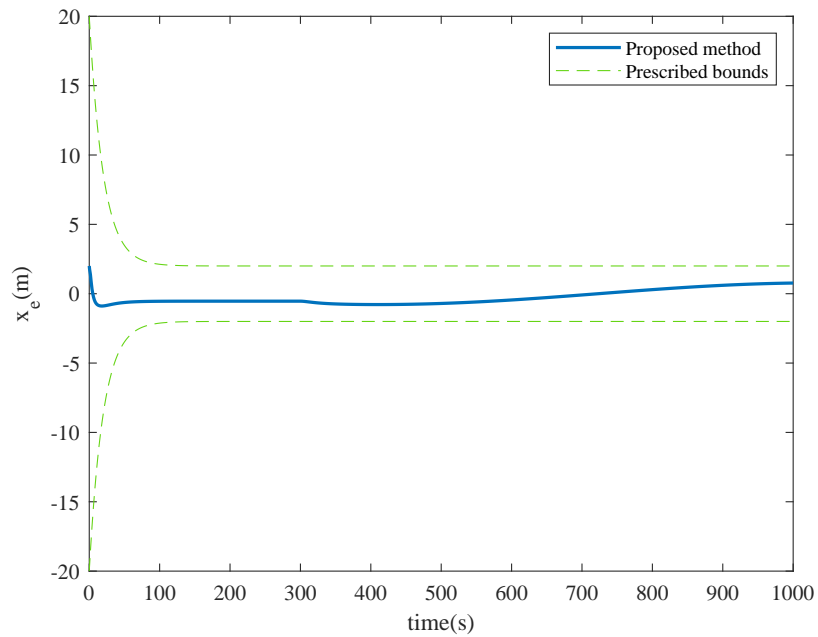
Figure 2. Trajectory tracking error of x.

Tables 1 and 2 show the control effects of the control methods proposed in this paper and those in other literature. By analyzing simulation results, it can be seen that the controller designed in this article has a good tracking performance when considering both preset performance and input quantization.

Figure 3. Trajectory tracking error of Y.

Figure 4. Trajectory tracking error of ψ.

Table 1. Numerical calculations were performed on the tracking error of the controller

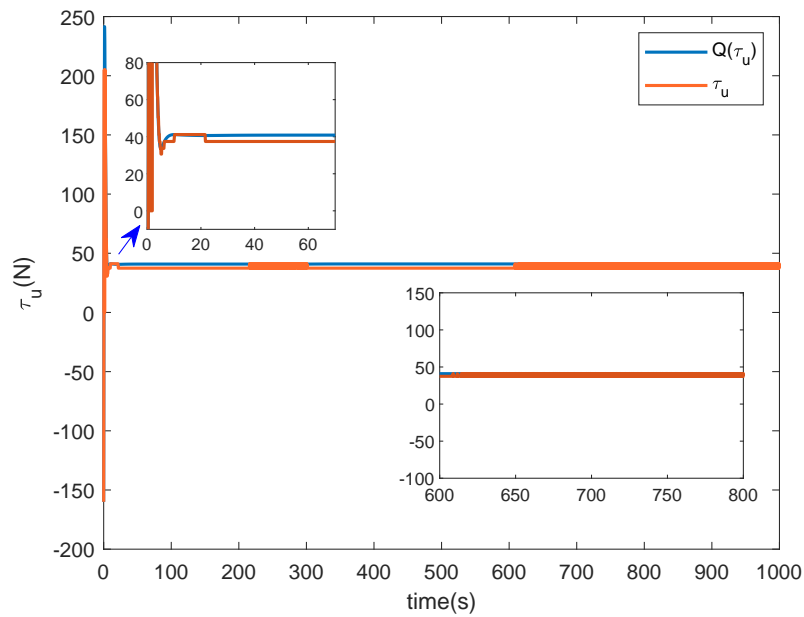| Tracking error \\ Time	5 s	10 s	20 s
x_e (m)	5.32	3.10	0.85
y_e (m)	6.42	4.58	1.17
ψ_e (rad)	0.84	0.65	0.42

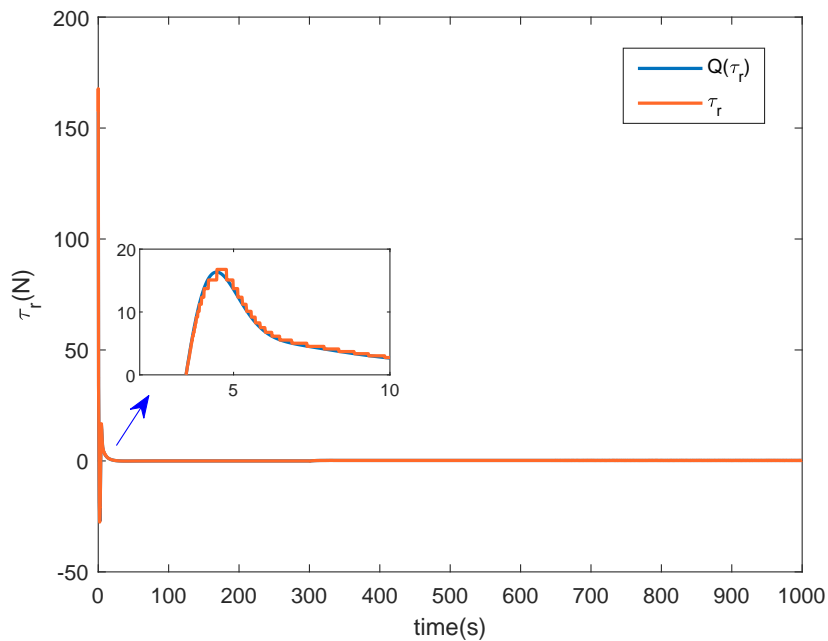**Figure 5.** Longitudinal control force.

Figure 6. Yaw control torque.

5. CONCLUSIONS

This article solves the trajectory tracking control problem of unmanned surface vessels by combining neural network technology, backstepping technology, and nonlinear mapping methods. In the design process of the controller, we simultaneously considered input quantization, constraints on preset performance, and the dynamic model of the real situation. The simulation results demonstrate the effectiveness of this method. In reality, there are problems such as input saturation and actuator failures, and the control method proposed in
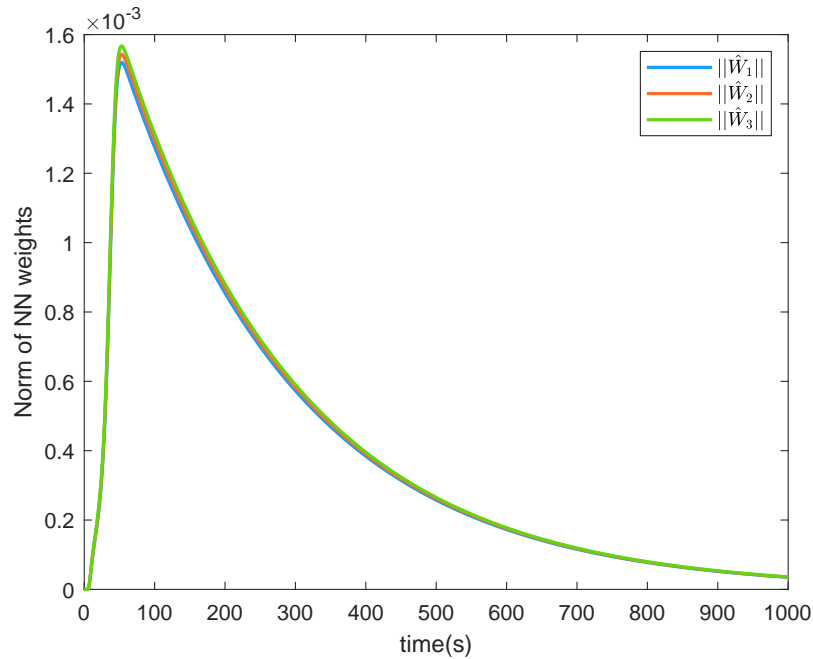
Figure 7. Neural network norm.

Table 2. Numerical calculations were performed on the tracking error of the controller [26]

Tracking error ＼ Time	5 s	10 s	20 s
x_e (m)	5.47	3.77	1.85
y_e (m)	6.81	5.23	2.04
ψ_e (rad)	0.92	0.74	0.51

this article currently cannot solve them. At present, fault-tolerant control [27–29] has a good effect on actuator faults in nonlinear systems. Therefore, further research will be conducted on how to utilize the robustness and learning ability of this method to address complex control problems such as control input saturation and partial actuator failures in underactuated surface unmanned systems.

DECLARATIONS

Authors' contributions
Conceptualization, methodology, writing - original draft, supervision: Zhang J
Software, visualization, data curation: Liu X
Writing - original draft, supervision: Wang X
Writing - reviewing and editing: Wang Y (Yang Wang)
Supervision: Wang Y (Yueying Wang)

Availability of data and materials
Data will be made available upon request.

and Technology, China (Grant No. 23010500100).

Conflicts of interest
Yueying Wang is an Editorial Board Member of the journal *Intelligence & Robotics*, while the other authors have declared that they have no conflicts of interest.

Ethics approval and consent to participate
Not applicable.

Consent for publication
Not applicable.

Copyright
© The Author(s) 2024.

REFERENCES

1. Patre BM, Londhe PS, Waghmare LM, Mohan S. Disturbance estimator based non-singular fast fuzzy terminal sliding mode control of an autonomous underwater vehicle. *Ocean Eng* 2018;159:372-87. DOI
2. Zhang Z, Shi Y, Zhang Z, Yan W. New results on sliding-mode control for takagi - sugeno fuzzy multiagent systems. *IEEE Trans Cybern* 2019;49:1592-604. DOI
3. Gao Z, Guo G. Fixed-time sliding mode formation control of AUVs based on a disturbance observer. *IEEE/CAA J Autom Sinica* 2020;7:539-45. DOI
4. Peng Z, Wang J, Wang J. Constrained control of autonomous underwater vehicles based on command optimization and disturbance estimation. *IEEE Trans Ind Electron* 2019;66:3627-35. DOI
5. Long L, Wang Z, Zhao J. Switched adaptive control of switched nonlinearly parameterized systems with unstable subsystems. *Automatica* 2015;54:217-28. DOI
6. He S, Dai S, Luo F. Asymptotic trajectory tracking control with guaranteed transient behavior for MSV with uncertain dynamics and external disturbances. *IEEE Trans Ind Electron* 2019;66:3712-20. DOI
7. Lin C, Wang H, Yuan J, Yu D, Li C. An improved recurrent neural network for unmanned underwater vehicle online obstacle avoidance. *Ocean Eng* 2019;189:106327. DOI
8. Wang J, Wang C, Wei Y, Zhang C. Command filter based adaptive neural trajectory tracking control of an underactuated underwater vehicle in three-dimensional space. *Ocean Eng* 2019;180:175-86. DOI
9. Ding L, Li S, Liu Y, Gao H, Chen C, Deng Z. Adaptive neural network-based tracking control for full-state constrained wheeled mobile robotic system. *IEEE Trans Syst Man Cybern Syst* 2017;47:2410-9. DOI
10. Xu B, Zhang R, Li S, He W, Shi Z. Composite neural learning-based nonsingular terminal sliding mode control of MEMS gyroscopes. *IEEE Trans Neural Netw Learn Syst* 2020;31:1375-86. DOI
11. Wei He, Zhao Yin, Changyin Sun. Adaptive neural network control of a marine vessel with constraints using the asymmetric barrier lyapunov function. *IEEE Trans Cybern* 2017;47:1641-51. DOI
12. Fan H, Tang J, Shi K, Zhao Y. Hybrid impulsive feedback control for drive-response synchronization of fractional-order multi-link memristive neural networks with multi-delays. *Fractal Fract* 2023;7:495. DOI
13. Dai SL, Wang M, Wang C, Li L. Learning from stable adaptive NN output feedback control of uncertain ship dynamics. In: Proceedings of the 31st Chinese Control Conference; 2012 Jul 25-27; Hefei, China. IEEE; 2012. pp. 5076-81. Available from: https://ieeexplore.ieee.org/document/6390821. [Last accessed on 12 Apr 2024]
14. Zhao Z, He W, Ge SS. Adaptive neural network control of a fully actuated marine surface vessel with multiple output constraints. *IEEE Trans Contr Syst Technol* 2014;22:1536-43. DOI
15. Dai S, Wang M, Wang C. Neural learning control of marine surface vessels with guaranteed transient tracking performance. *IEEE Trans Ind Electron* 2016;63:1717-27. DOI
16. He W, Chen Y, Yin Z. Adaptive neural network control of an uncertain robot with full-state constraints. *IEEE Trans Cybern* 2016;46:620-9. DOI
17. Bechlioulis CP, Karras GC, Heshmati-Alamdari S, Kyriakopoulos KJ. Trajectory tracking with prescribed performance for underactuated underwater vehicles under model uncertainties and external disturbances. *IEEE Trans Contr Syst Technol* 2017;25:429-40. DOI
18. Elhaki O, Shojaei K. Neural network-based target tracking control of underactuated autonomous underwater vehicles with a prescribed performance. *Ocean Eng* 2018;167:239-56. DOI
19. Shojaei K, Dolatshahi M. Line-of-sight target tracking control of underactuated autonomous underwater vehicles. *Ocean Eng* 2017;133:244-52. DOI
20. Shao X, Si H, Zhang W. Fuzzy wavelet neural control with improved prescribed performance for MEMS gyroscope subject to input

quantization. *Fuzzy Set Syst* 2021;411:136-54. DOI

21. Huang B, Zhou B, Zhang S, Zhu C. Adaptive prescribed performance tracking control for underactuated autonomous underwater vehicles with input quantization. *Ocean Eng* 2021;221:108549. DOI

22. Park BS, Kwon J, Kim H. Neural network-based output feedback control for reference tracking of underactuated surface vessels. *Automatica* 2017;77:353-9. DOI

23. Zhou J, Wen C, Yang G. Adaptive backstepping stabilization of nonlinear uncertain systems with quantized input signal. *IEEE Trans Automat Contr* 2014;59:460-4. DOI

24. Chen L, Cui R, Yang C, Yan W. Adaptive neural network control of underactuated surface vessels with guaranteed transient performance: theory and experimental results. *IEEE Trans Ind Electron* 2020;67:4024-35. DOI

25. Yoo SJ, Park BS. Guaranteed performance design for distributed bounded containment control of networked uncertain underactuated surface vessels. *J Frank Inst* 2017;354:1584-602. DOI

26. Zhong Y, Weng L, Xu L. Adaptive sliding mode trajectory tracking control of incomplete symmetry underactuated USV. *Ship Sci Technol* 2020;42:92-8. (in Chinese) DOI

27. Zhang G, Huo X, Liu J, Ma K. Adaptive control with quantized inputs processed by lipschitz logarithmic quantizer. *Int J Control Autom Syst* 2021;19:921-30. DOI

28. Zhang X, Xu X, Li J, et al. Observer-based H_∞ fuzzy fault-tolerant switching control for ship course tracking with steering machine fault detection. *ISA Trans* 2023;140:32-45. DOI

29. Xiong J, Li J, Du P. A novel non-fragile H_∞ fault-tolerant course-keeping control for uncertain unmanned surface vehicles with rudder failures. *Ocean Eng* 2023;280:114781. DOI